Trauma Monthly 2022; Covid-19 & Emergency Medicine (Special Issue 1): 54-67

10.30491/TM.2021.310669.1386

Trauma Monthly

Original Article

Clinical, Laboratory, and Chest CT Scan Prognostic Factors for COVID-19 Mortality Cases

Dina Jalalvand [1], Fatemeh Akbari [1], Ali Pirsalehi [2], Pooneh Dehghan [1], Seyed Aria Nejadghaderi [3], Laya Jaliliankhave [3], Taha Hasanzadeh [3], Ghazal Sanadgol [3], Dorsa Shirini [3], Zeinab Eslami [1*]

[1] Radiology department, Taleghani hospital, Shahid Beheshti University of medical sciences, Tehran, Iran.

[2] Internal Medicine Department, School of Medicine, Shahid Beheshti University of medical sciences, Tehran, Iran.

[3] School of Medicine, Shahid Beheshti University of Medical Sciences, Tehran, Iran.

*Corresponding Author: Zeinab Eslami, Medical Student, Radiology Department, Taleghani hospital, Shahid Beheshti University of medical sciences, Tehran, Iran, E-mail: mypillarbox@ymail.com.

Received 2020-01-28; **Accepted** 2021-10-05; **Online Published** 2021-12-29

Abstract

Introduction: World Health Organization (WHO) declared a novel HCoVs (COVID-19) to be a public health emergency of international concern on 30 January, 2020. Typical clinical symptoms of patients include fever, dry cough, breathing difficulties (dyspnea). CT is the most sensitive radiological technique for the diagnosis of COVID-19, showing spectrum of lung features. The purpose of this study was to investigate clinical and laboratory outcomes and chest CT futures of patients to recognize prognostic factors for COVID-19.

Methods: Clinical and laboratory findings and chest CT futures were evaluated from 226 admitted patients with the initial diagnosis of COVID-19 who were recovered or died due to the disease and its complications. The association between vital status and categorical variables was evaluated. The single and multiple logistic models were used for assessing the impact of study variables on the hazard of occurring death.

Results: The prediction power of some variables were significant. The highest AUCs were observed for GGO pattern, age, lymphocyte count, Creatinine, CRP, LDH, and Systolic Blood Pressure. This study was reached an accurate for predicting vital status among COVID-19 patients.

Conclusion: In this study, we evaluated and presented CT feature parameters as well as clinical and laboratory markers as a model that predicts vital status among COVID-19 patients.

Keywords: COVID-19; Mortality; Computed Tomography; Ground-Glass Opacity.

Introduction

Human coronaviruses (HCoVs) were first described in the 1960s for patients with the common cold. Since then, more HCoVs have been discovered, including those that cause severe acute respiratory syndrome (SARS) and the Middle East respiratory syndrome (MERS), two pathogens that, upon infection, can cause fatal respiratory disease in humans [1-7].

World Health Organization (WHO) declared a novel HCoVs (COVID-19) to be a public health emergency of international concern on 30 January, 20202. The identification of the new pathogen along with many unknowns. 16 July 2020, about 216 countries, 13,378,853 cases of COVID-19 and 580045 deaths with an average mortality of about 4.5 % have been reported all throughout the world 8. It is lower than that of severe acute respiratory syndrome (SARS)5 and the Middle East respiratory syndrome (MERS)6. However, the mortality is significantly high in critically patients with COVID-19 (62%), and older patients with comorbidities are at increased risk of developing

critical illness and death[7].

Typical clinical symptoms of patients are fever, dry cough, breathing difficulties (dyspnea), headache, and pneumonia. Disease onset may result in progressive respiratory failure owing to alveolar damage (as observed by transverse chest computerized tomography images) and even death[3].

Imaging plays a crucial role in the diagnosis and evaluation of the disease. Although, diagnosis relies on Real-Time Reverse-Transcriptase-Polymerase Chain Reaction (RT-PCR) positivity for the presence of coronavirus. The sensitivity of the initial CT scan is about 97.2%, whereas the initial RT-PCR sensitivity is 83.3%10. The average time from initial disease onset to CT scan was 3 +/- 3 days, and this time for RT-PCR testing was 3 +/- 3 days11. Research results supported the use of chest CT scan for screening COVID-19 in patients with clinical and epidemiologic features compatible with COVID-19 infection, especially when RT-PCR testing is negative [11].

Also, chest CT had high sensitivity for the diagnosis of COVID-19 and should be considered for the COVID-19 screening, comprehensive evaluation, and following-up, especially in epidemic areas with a high pre-test probability for disease. Since patients with negative RT-PCR tests, more than 80% had typical CT scan manifestations. Therefore, they were re-classified as highly likely or probable cases with COVID-19, by the comprehensive analysis of clinical symptoms, usual CT manifestations, and dynamic CT scan follow-ups[12].

Computed tomography (CT) is the most sensitive radiological technique for the diagnosis of COVID-19, showing diffuse lung alterations ranging from ground-glass opacities to parenchymal consolidations; several radiological patterns are observed at different times throughout the disease course4. Among the patients, about one-fifth required intensive care unit (ICU), one-third presented with acute respiratory distress syndrome (ARDS), and about 6% with shock. The case fatality rate among hospitalized patients is more than 10%[13]. The clinical and laboratory pictures of SARS, MERS, and COVID-19 seem similar despite there are differences in the early reports[13]. A complete clinical characterization of COVID-19 infection, such as its laboratory and image markers, is required.

The study aimed to investigate clinical and laboratory findings and chest CT Futures of mortality cases due to COVID-19.

Methods

This study received medical ethical committee approval, and the requirement for patient informed consent was waived under Council for International Organization of Medical Science guidelines.

Patient Population and Study Design

In this retrospective study, we enrolled cases with clinical manifestation of COVID-19 whose disease was confirmed by RT-PCR assay on the nasopharyngeal swabs.

All patients were admitted at Taleghani Hospital, an urban multicenter health system, from March 2020 to the end of April 2020. All patients were confirmed by at least two positive results of RT-PCR or future highly suggestive chest CT scan for COVID-19 infection.

Inclusion criteria were (a) patients with fever and respiratory symptoms, (b) patients with mild respiratory symptoms, and close contact with a confirmed COVID-19 patient.

Exclusion criteria were (a) chest Ct scan with IV contrast performed for vascular indication such as pulmonary embolism, aortic dissection, etc., (b) severe chest CT motion artifact.

Finally, 226 cases were included in the study. The patients were divided into two groups of recovered and death categories.

Clinical and Laboratory Data

Clinical and initial laboratory data were collected from electronic hospital information system. They contain patient demographic characteristics, initial

symptoms, history of close contact with a confirmed COVID-19 disease, past medical history and drug history. Also, initial clinical signs including vital sign, temperature, pulse oxy oxymetrymethry, Glasco Coma Score, and hematologic and other laboratory data were collected. Fever was defined with a temperature over 37.5 C. Other Information during hospitalization were overall hospitalization duration and need for ICU admission or intubation procedure were collected thus.

CT Acquisition Technique

All chest CT scans were obtained without any contrast medium, with the patients in the supine position and full inspiration, from top of shoulder through the mid-liver level. Patients underwent scanning with Somatom Emotion (Siemens Healthcare) by acquisition parameters of 120 kVp, tube current modulation 100-200 mAs, spiral pitch factor 0.75-1.5, and collimation width 0.625-5 mm. Imaging data were reconstructed at a slide thickness of 0.625-5mm by a Medium Sharp Reconstruction Algorithm. All decontamination protocols were completely done.

CT Image Analysis

DICOM data were transferred onto a PACS workstation. Two radiologists with 8 and 6 years of thoracic imaging experience reviewed CT scans blindly in at least both lung (width, 1500HU, level -700 HU) and mediastinal (width 350 HU, level 40 HU) settings. The CT scans were described with features that include ground-glass opacity (GGO), consolidation, nodular pattern, architectural distortion, crazy paving, cavitation, revers halo sign, traction bronchiectasis, and intraseptal thickening. Additional findings contained intrathoracic, lymph node enlargement, pleural effusion, cardiomegaly and main pulmonary artery enlargement. The distributions were evaluated as five: axial, diffuse, peribronchovascular, pleural based peripherally, and pleural spared peripherally type. We also described lobar involvement pattern as one lobe, bilateral (both lungs), multilobar in one lung and all five lobes involvement. We described every Five lobes' involvement percentage as five scores: zero for no involvement, 5 for lower than 25%, 4 for 26-50%, 3 for 51-75%, and 2 or 1 for more than 76% involvement. Finally, all CT scans were divided into three consequences as highly suggestive, indeterminate or inconsistent with COVID-19.

Statistical Analysis

Statistical analysis was performed using SPSS version 21.0. Descriptive statistics were presented using median (Q1, Q3) and frequency (percentage) for numeric and categorical variables. All comparisons of numeric variables between categories of vital status were performed using the Mann-Whitney U test. The association between criticalstatus and categorical variables was evaluated using the Pearson chi-square test or Fisher exact test. The single and multiple logistic models were used for evaluating the impact of study variables on the hazard of occurring death. The area under the ROC curve (AUC), sensitivity (SE), specificity (SP), positive predictive value (PPV), negative predictive value (NPV), and accuracy were used to show the prediction power of variables for predicting the vital status in logistic regression. Significant variables for the prediction of vital status were determined using the Boruta method. All analyzes were done using R (version 4.0.2) and SPSS (version 27.0). P-values less than 0.05 were considered statistically significant.

Results

A total of 256 admitted patients with the initial diagnosis of COVID-19 were enrolled in the research who were admitted to Taleghani multicenter health system. Thirty patients were excluded due to exclusion criteria. Finally, there was 226 patients, including 119 males and 107 females (mean age 57.8±16.6 y, range 19-94). All patients had a spectrum of clinical findings and symptoms suspected for COVID-19 disease. Fifty-

eight patients were died due to the disease and its complications. No significant differences were identified in sex distribution (p=0.64), whereas recovered patients were significantly younger than deceased ones (p<0.001) (Table 1).

Clinical characteristic

All clinical data were collected at the admit time. Totally 124 (54.6%) patients had a positive past medical history, had suffered from hypertension (37%), ischemic heart disease (37%), cancer (30.8%). including ten lymphoma cases, diabetes mellitus (29.2%) and chronic pulmonary disease (12.3%). Seventeen patients (7.5%) had positive smoking history and 7.7% were drug abusers. Positive drug history was 13.8% for b-Blockers, 15.4% for ARB, and 9.2% for ACE inhibitors. 6 cases had taken corticosteroid recently. 2 pregnant patients had been in the cases.

The average hospitalization duration was 7.7±9 days, and 38.7% of cases were admitted to ICU. 30% of patients had invasive endotracheal intubation with an average period of 2.3±5.6 days (range 0-40). 35.4% of cases had a 1-day duration. The most frequent late complication was ARDS (69%) and ARDS+AKI (10%). Three patients have experienced cardiac arrhythmia and arrest. The most common clinical features were dyspnea (104 cases, 46%), fever (97 cases, 42.9%), cough (91 cases, 40%), anorexia (61 cases, 27.5%), nausea/vomiting (47 cases, 21.5%), general abdominal pain (40 cases, 18.5%), chill (43 cases, 19%) and myalgia (29cases, 13%). Mean systolic blood pressure was 122±38, and diastolic blood pressure of 76±12. Initial O2 saturation was 89.62 % (range 50-99%). The mean sublingual body temperature was 37.48±0.8 ˚c (range 36.5-40˚c). The mean Glasco Coma Score was 13.9±3 (range 3-15). Mean heart rate was 87±48 /min, and mean respiratory rate was 18±01 /min. Mean Symptoms onset to die duration was 10±10 days (range1-50 d), and mean duration of hospitalization was 8±9 days (range 1-49 d).

Laboratory data

All laboratory findings were from samples taken at admitting time or during the first day of hospitalization utmost. Mean HCT was 30±8 % (range 11.4-54). The mean RBC count was 3.5±1.1 $\times 10^6/\mu l$ (range 1-8.1) with mean hemoglobin of 10.9±2.5 mg/dl (range4-18). The mean Platelets count was 203±106 $\times 10^3/\mu l$ (range 1-666). Mean WBC count was 9.12±10.6 $\times 10^3/\mu l$ (range 0.2-98). WBC differentiation were thus: Mean neutrophil percentage was 79.5 ± 15% (range 20-95%), mean lymphocyte percentage was 14.7 ± 14.7% (range 3-76) and mean monocyte percentage was 5.5 ± 5% (range 1-23). Mean CRP was 45.9 ±47 (range 1-218), mean LDH level was 657 ±416 (range78-3287), and mean ESR was 36.8 ±24 (range 3-109). Mean AST level was 56.9 ±74.9, Mean ALT level was 66 ± 120 (range 7-795), mean ALP level was 387 ±487 (range 88-2255), and mean INR was 1.3±0.6 (range 1-5.4). Mean arterial blood gas pH was 7.27 ±0.51 (range 7.1-7.5).

CT Findings

All patients underwent chest CT scans in the first 24 hours of admission. Three major parenchymal involvement patterns based on prior studies were evaluated. Ground glass opacity was seen in 169 patients (74.7%), consolidation in 30%, and nodular pattern only in 4.4% of cases. Other patterns were included crazy paving (10.6%), parenchymal bands (2.2%), reverse halo sign (1.8%), and emphysema (1.3%). Peripheral distribution was the most common distribution (58%), followed by a diffuse pattern in 35.4%. Pleural effusion was seen in 32 patients (14.2%), and pulmonary hypertension based on main pulmonary artery diameter was seen in 9.3%.

Patterns of the lesions

The results revealed that the GGO and consolidation were significantly higher in CT images of the deceased group. In addition, the incidence of nodules showed a remarkably higher rate in dead patients in all lung lobes except for the

LUL (p=0.999). Per lymphatic nodules were just found in the RUL of one patient in the deceased group. Two patients in each group showed reverse halo signs in their CT scans. There were factors including architectural distortion, parenchymal band, cavity, pleural/pericardial effusion, and pulmonary hypertension (HTN) in the deceased patients. On the other hand, only one recovered patient showed pulmonary fibrosis, and it did not identify in images of deceased participants. There were no pulmonary masses, lymphadenopathy, or bronchiectasis in our enrolled participants.

Distribution of the lesions

The most common distribution pattern of lung lobes involvements in the deceased group was diffuse. However, the peripheral and pleural based pattern had the highest prevalence in CT findings of the recovered patients. No patient in the recovered group showed peripheral and pleural sparing and peribronchovascular patterns. Also, the axial distribution pattern was not identified in RUL, RML, and LUL of deceased patients. Table 3 shows the frequency of different patterns of distribution in each lobe of the lung by the group.

Fifty-eight patients died from COVID-19, with a significantly higher median age than those who survived (53.50 vs. 65.0 years, p<0.001). all descriptive statistic for categorical and numeric variables were presented in Table 2. Accordingly, the relation between vital status and variables including age (p<0.001), co-morbidity (p=0.006), PaO2 (p=0.016), Systolic Blood Pressure (p=0.010), WBC (p=0.001), Hemoglobin (p<0.001), lymphocyte count (p<0.001), Creatinine (p<0.001), AST (p=0.008), ESR (p=0.035), CRP (p=0.001), LDH (p<0.001), VBG PH (p=0.020), Ground Glass Opacity(GGO) (p<0.001), Consolidation pattern (p<0.001), CT-scan pattern (p<0.001), lesion distribution (p<0.001), and pleural effusion (p<0.001) were significant.

The results of single and multiple analyses were presented in Table 3. Higher values of variables including age (OR: 1.06, p<0.001), co-morbidity (Or: 1.37, p=0.026), AST (OR=1.01, p=0.004), ESR (OR=1.01, p=0.045), CRP (OR=1.01, p=0.002), LDH (OR=1.00, p=0.006), and INR (OR=1.98, p=0.024) were associated with higher hazard of occurring death. In addition, indeterminate CT-scan vs. normal CT-scan (OR=6.79, p=0.001), diffuse distribution vs. peripheral (OR=4.38, p<0.001), and pleural effusion were related with a higher risk of death. However, lower hazard of death was observed in higher values of PaO2 (OR=0.91, p<0.001), SBP (OR=0.98, p=0.050), Hb (OR=0.75, p<0.001), and lymph (OR=0.93, p=0.001).

The prediction power of total explanatory variables was summarized in Table 3. The highest AUCs were observed for variables of GGO (0.96), age (0.79), lymph (0.79), Cr (0.76), CRP (0.76), LDH (0.75), and Systolic Blood Pressure (0.71). The importance of variables is shown in Figure 1. Accordingly, the high score ground-glass opacity was the most important variable for the prognosis of the vital status of patients with COVID-19. Additionally, all variables highlighted in green boxes played an important role in predicting vital status. In the last step, two subsets of predictors were chosen for predicting vital status. The difference between the two models was in the presence or absence of GGO. In the first model, the correct classification was done. But in the second model, without the presence of the GGO variable, the AUC was 0.84. As a result, the second model was the most accurate for predicting vital status among COVID-19 patients, as the overfitting was much lower than in the first model (Table 4).

Table 1. Distribution patterns of lung involvement by lung lobes in each group.

	Area	Deceased		Recovered		P-value
		N	Percent	N	Percent	
RUL	Axial	0	0.0%	5	5.4%	<0.0001
	Diffuse	32	71.1%	32	34.4%	
	Peribronchovascular	2	4.4%	0	0.0%	
	Peripheral, Pleural Based	9	20.0%	56	60.2%	
	Peripheral, Pleural Sparing	2	4.4%	0	0.0%	
RML	Axial	0	0.0%	4	5.3%	<0.0001
	Diffuse	28	80.0%	29	38.2%	
	Peribronchovascular	1	2.9%	0	0.0%	
	Peripheral, Pleural Based	6	17.1%	43	56.6%	
	Peripheral, Pleural Sparing	0	0.0%	0	0.0%	
RLL	Axial	2	4.4%	5	4.7%	<0.0001
	Diffuse	30	66.7%	31	29.0%	
	Peribronchovascular	3	6.7%	0	0.0%	
	Peripheral, Pleural Based	9	20.0%	71	66.4%	
	Peripheral, Pleural Sparing	1	2.2%	0	0.0%	
LUL	Axial	0	0.0%	6	5.7%	<0.0001
	Diffuse	33	73.3%	29	27.6%	
	Peribronchovascular	4	8.9%	0	0.0%	
	Peripheral, Pleural Based	8	17.8%	70	66.7%	
	Peripheral, Pleural Sparing	0	0.0%	0	0.0%	
LLL	Axial	2	4.4%	3	2.9%	<0.0001
	Diffuse	35	77.8%	31	30.1%	
	Peribronchovascular	1	2.2%	0	0.0%	
	Peripheral, Pleural Based	6	13.3%	69	67.0%	
	Peripheral, Pleural Sparing	1	2.2%	0	0.0%	

Abbreviations: RUL: right upper lobe; RML: right middle lobe; RLL: right lower lobe; LUL: left upper lobe; LLL: left lower lobe; OR: odds ratio; N: number

Table 2. Descriptive statistics of study variables by vital status (death or survivor)

Variables	Levels	Total (N=226)	Status		P-value
			Survived (N=168)	Deceased (N=58)	
Age		58.50 (45.75, 70.0)	53.50 (42.0, 68.0)	65.0 (58.75, 74.75)	<0.001
Comorbidity		2.0 (1.0, 3.0)	1.0 (1.0, 3.0)	2.0 (1.0, 3.0)	0.006
PaO2		91.0 (88.0, 94.0)	92.0 (89.0, 94.0)	89.0 (78.0, 94.0)	0.016
SBP		120.0 (110.0, 130.0)	121.0 (110.0, 130.0)	115.0 (100.0, 130.0)	0.01
DBP		78.5 (70.0, 80.0)	80.0 (70.0, 80.0)	70.0 (64.0, 80.0)	0.094
HR		85.5 (80.0, 95.0)	86.0 (80.0, 94.0)	84.0 (80.0, 96.5)	0.924
RR		18.0 (16.0, 19.0)	18.0 (17.0, 19.0)	18.0 (16.0, 20.0)	0.933
Temperature		37.2 (37.0, 38.0)	37.3 (37.0, 38.0)	37.0 (37.0, 37.8)	0.447
WBC		6.5 (4.5, 9.5)	6.0 (4.5, 8.7)	9.5 (5.6, 14.7)	0.001
PLT		188.0 (139.0, 261.0)	184.0 (145.0, 250.0)	197.5 (102.5, 298.8)	0.961
Hb		11.4 (9.5, 12.8)	11.7 (10.1, 13.0)	9.7 (8.3, 11.5)	<0.001
Lymph		18.0 (10.8, 26.0)	20.0 (13.8, 27.0)	10.0 (7.0, 15.8)	<0.001
Cr		1.0 (0.8, 1.3)	1.0 (0.8, 1.2)	1.4 (1.0, 2.6)	<0.001
AST		37.0 (26.8, 56.3)	35.0 (24.0, 50.0)	46.0 (31.5, 88.5)	0.008
ESR		30.0 (17.0, 51.3)	27.0 (14.3, 49.0)	39.0 (20.0, 65.0)	0.035
CRP		26.0 (11.0, 73.3)	22.0 (10.0, 47.0)	64.5 (18.3, 96.0)	0.001
LDH		549.0 (438.0, 689.3)	492.5 (409.3, 645.8)	675.5 (532.8, 961.0)	<0.001
INR		1.2 (1.1, 1.4)	1.2 (1.0, 1.3)	1.3 (1.1, 1.7)	0.002
PH		7.3 (7.3, 7.4)	7.3 (7.3, 7.4)	7.3 (7.2, 7.3)	0.020
GGO		2.0 (1.0, 3.0)	3.0 (2.0, 3.0)	1.0 (1.0, 1.0)	<0.001
Consolidation		1.0 (1.0, 1.0)	1.0 (1.0, 2.0)	1.0 (1.0, 1.0)	<0.001
Nodular		1.0 (1.0, 1.0)	1.0 (1.0, 1.0)	1.0 (1.0, 1.0)	0.284
	No	216 (95.6)	162 (96.4)	54 (93.1)	
	Yes	10 (4.4)	6 (3.6)	4 (6.9)	
CT-Scan					<0.001[a]
	Highly Suggestive	162 (71.7)	118 (70.2)	44 (75.9)	
	Inconsistent	23 (10.2)	20 (11.9)	3 (5.2)	
	Indeterminate	15 (6.6)	5 (3.0)	10 (17.2)	
	Normal	26 (11.5)	25 (14.9)	1 (1.7)	
			5 (2.98)	10 (17.24)	
PCR	No	55 (40.74)	44 (41.12)	11 (39.29)	0.860[a]
	Yes	80 (59.26)	63 (58.88)	17 (60.71)	
Sex	Male	123 (54.40)	92 (54.80)	31 (53.40)	0.863[a]
	Female	103 (45.60)	76 (45.20)	27 (46.60)	
Fever	No	83 (45.86)	52 (41.94)	31 (54.39)	0.118[a]
	Yes	98 (54.14)	72 (58.06)	26 (45.61)	
Cough	No	91 (50)	57 (45.6)	34 (59.65)	0.079[a]
	Yes	91 (50)	68 (54.4)	23 (40.35)	
Dyspnea	No	76 (42.22)	51 (41.46)	25 (43.86)	0.762[a]
	Yes	104 (57.78)	72 (58.54)	32 (56.14)	
Smoke	No	165 (90.66)	112 (89.6)	53 (92.98)	0.467[a]
	Yes	17 (9.34)	13 (10.4)	4 (7.02)	
Distribution					<0.001[b]
	Axial	10 (4.4)	6 (3.6)	4 (6.9)	
	Peribronchovascular	5 (2.2)	0 (0.0)	5 (8.6)	
	Diffuse	70 (31.0)	35 (20.8)	35 (60.3)	
	peripheral	98 (43.4)	86 (51.2)	12 (20.7)	
			35 (27.56)	35 (62.5)	
Pleural effusion	No	194 (85.84)	158 (94.05)	36 (62.07)	<0.001[a]
	Yes	32 (14.16)	10 (5.95)	22 (37.93)	
PHTN	No	205 (90.71)	156 (92.86)	49 (84.48)	0.058[a]
	Yes	21 (9.29)	12 (7.14)	9 (15.52)	

Note: all comparison of numeric variables between categories of status were performed using Mann-Whitney U test. The association between vital status and categorical variables were evaluated using a) Pearson chi-square test or b) Fisher exact test.

Abbreviations: Systolic blood pressure (SBP), Diastolic blood pressure (DBP), Heart rate (HR), Respiratory rate (RR), White Blood Cell (WNC), Platelet (PLT), Hemoglobin (Hb), Creatinine (Cr), Aspartate aminotransferase (AST), Erythrocyte sedimentation rate (ESR), C-reactive protein (CRP), Lactate dehydrogenase (LDH), International normalized ratio (INR), Ground glass (GGO)

Table 3. The single and multiple impact of variables on the odds of occurring death

		Univariate		Multiple	
Variables	**Levels**	**OR (95% CI)**	**P-value**	**OR (95% CI)**	**P-value**
Age		1.06 (1.04, 1.08)	<0.001		
Comorbidity		1.37 (1.04, 1.83)	0.026	1.95 (1.19, 3.21)	0.009
PaO2		0.91 (0.87, 0.96)	<0.001	0.89 (0.82, 0.96)	0.005
SBP		0.98 (0.97, 1.00)	0.050		
DBP		0.98 (0.95, 1.01)	0.208		
HR		1.00 (0.98, 1.02)	0.873		
RR		1.01 (0.90, 1.12)	0.923		
Temperature		0.83 (0.54, 1.22)	0.351		
WBC		1.02 (1.00, 1.06)	0.079		
PLT		1.00 (1.00, 1.00)	0.478		
Hb		0.75 (0.65, 0.86)	<0.001	0.70 (0.53, 0.92)	0.011
Lymph		0.93 (0.89, 0.97)	0.001		
Cr		1.06 (0.95, 1.19)	0.277		
AST		1.01 (1.00, 1.02)	0.004	1.02 (1.00, 1.03)	0.024
ESR		1.01 (1.00, 1.03)	0.045		
CRP		1.01 (1.00, 1.02)	0.002		
LDH		1.00 (1.00, 1.00)	0.006		
INR		1.98 (1.15, 3.88)	0.024		
PH		1.03 (0.56, 3.50)	0.939		
GGO		0.00 (0.00, NA)	0.992		
Consolidation		0.00 (NA, NA)	0.993		
Nodular					
	No (Reference)	-----	-----		
	Yes	2.00 (0.50, 7.27)	0.297		
CT-Scan					
	Highly Suggestive	1.33 (0.68, 2.72)	0.413		
	Inconsistent	0.40 (0.09, 1.24)	0.156		
	Indeterminate	6.79 (2.30, 22.70)	0.001		
	Normal (Reference)				
PCR	No (Reference)				
	Yes	1.08 (0.47, 2.59)	0.86		
Sex	Male (Reference)				
	Female	1.05 (0.58, 1.92)	0.863		
Fever	No (Reference)				
	Yes	0.61 (0.32, 1.14)	0.12		
Cough	No (Reference)				
	Yes	0.57 (0.30, 1.07)	0.08		
Dyspnea	No (Reference)				
	Yes	0.91 (0.48, 1.72)	0.762		
Smoke	No (Reference)				
	Yes	0.65 (0.18, 1.94)	0.47		
Distribution					
	Axial	1.55 (0.38, 5.66)	0.51		
	Peribronchovascular	NA (0.00, NA)	0.987		
	Diffuse	4.38 (2.27, 8.65)	<0.001		
	peripheral (Reference)				
Pleural effusion	No (Reference)				
	Yes	9.66 (4.31, 23.02)	<0.001		
PHTN	No (Reference)				
	Yes	2.39 (0.92, 5.98)	0.064		

Note: The Backward method with Wald statistic was used to select variables. All correlated predictors were removed from the multiple model to avoid the multicollinearity problem.

Abbreviations: Systolic blood pressure (SBP), Diastolic blood pressure (DBP), Heart rate (HR), Respiratory rate (RR), White Blood Cell (WNC), Platelet (PLT), Hemoglobin (Hb), Creatinine (Cr), Aspartate aminotransferase (AST), Erythrocyte sedimentation rate (ESR), C-reactive protein (CRP), Lactate dehydrogenase (LDH), International normalized ratio (INR), Ground glass (GGO)

Table 4. The predictive power of study variables for prediction of vital status

Variables	AUC (95% CI)	Cut-off	SE (95% CI)	SP (95% CI)	PPV (95% CI)	NPV (95% CI)	Accuracy 95% CI)
Age	0.79 (0.65, 0.93)	0.29	0.83 (0.52, 0.98)	0.63 (0.49, 0.75)	0.32 (0.21, 0.82)	0.95 (0.79, 0.97)	0.66 (0.54, 0.77)
Comorbidity	0.59 (0.39, 0.80)	0.47	0.25 (0.03, 0.65)	0.90 (0.73, 0.98)	0.81 (0.30, 0.96)	0.81 (0.30, 0.96)	0.78 (0.62, 0.90)
PaO2	0.60 (0.34, 0.86)	0.31	0.50 (0.19, 0.81)	0.85 (0.72, 0.93)	0.90 (0.67, 0.96)	0.90 (0.67, 0.96)	0.81 (0.69, 0.90)
SBP	0.71 (0.51, 0.90)	0.31	0.67 (0.35, 0.90)	0.75 (0.61, 0.85)	0.91 (0.73, 0.95)	0.91 (0.73, 0.95)	0.70 (0.58, 0.81)
DBP	0.57 (0.38, 0.76)	0.33	0.25 (0.05, 0.57)	0.93 (0.82, 0.98)	0.85 (0.50, 0.96)	0.85 (0.50, 0.96)	0.81 (0.69, 0.89)
HR	0.42 (0.21, 0.63)	0.34	0.09 (0.00, 0.41)	1.00 (0.93, 1.00)	0.84 (0.11, 1.00)	0.84 (0.11, 1.00)	0.83 (0.72, 0.91)
RR	0.48 (0.27, 0.68)	0.27	0.89 (0.52, 1.00)	0.17 (0.08, 0.31)	0.89 (0.52, 0.95)	0.89 (0.52, 0.95)	0.24 (0.13, 0.37)
Temperature	0.57 (0.41, 0.73)	0.27	0.70 (0.35, 0.93)	0.58 (0.44, 0.72)	0.91 (0.70, 0.95)	0.91 (0.70, 0.95)	0.56 (0.42, 0.68)
WBC	0.67 (0.44, 0.91)	0.29	0.64 (0.31, 0.89)	0.85 (0.73, 0.94)	0.92 (0.75, 0.97)	0.92 (0.75, 0.97)	0.82 (0.70, 0.90)
PLT	0.59 (0.35, 0.83)	0.28	0.55 (0.23, 0.83)	0.80 (0.66, 0.89)	0.90 (0.69, 0.95)	0.90 (0.69, 0.95)	0.17 (0.09, 0.28)
Hb	0.62 (0.42, 0.83)	0.35	0.64 (0.31, 0.89)	0.76 (0.63, 0.87)	0.91 (0.73, 0.96)	0.91 (0.73, 0.96)	0.74 (0.62, 0.84)
Lymph	0.79 (0.62, 0.96)	0.33	0.78 (0.40, 0.97)	0.82 (0.69, 0.92)	0.95 (0.80, 0.98)	0.95 (0.80, 0.98)	0.82 (0.70, 0.90)
Cr	0.76 (0.62, 0.89)	0.28	1.00 (0.72, 1.00)	0.44 (0.30, 0.59)	1.00 (0.83, 1.00)	1.00 (0.83, 1.00)	0.18 (0.09, 0.30)
AST	0.59 (0.36, 0.82)	0.29	0.73 (0.39, 0.94)	0.63 (0.48, 0.77)	0.91 (0.70, 0.95)	0.91 (0.70, 0.95)	0.65 (0.51, 0.77)
ESR	0.49 (0.26, 0.71)	0.45	0.20 (0.03, 0.56)	1.00 (0.92, 1.00)	0.85 (0.37, 1.00)	0.85 (0.37, 1.00)	0.86 (0.74, 0.94)
CRP	0.76 (0.63, 0.90)	0.26	1.00 (0.69, 1.00)	0.49 (0.34, 0.64)	1.00 (0.84, 1.00)	1.00 (0.84, 1.00)	0.58 (0.44, 0.71)
LDH	0.75 (0.60, 0.90)	0.35	0.86 (0.42, 1.00)	0.68 (0.51, 0.82)	0.96 (0.76, 0.98)	0.96 (0.76, 0.98)	0.71 (0.56, 0.84)
INR	0.52 (0.25, 0.78)	0.55	0.44 (0.14, 0.79)	0.86 (0.72, 0.95)	0.88 (0.59, 0.96)	0.88 (0.59, 0.96)	0.77 (0.63, 0.87)
PH	0.43 (0.19, 0.66)	0.31	0.30 (0.07, 0.65)	0.78 (0.64, 0.89)	0.84 (0.46, 0.92)	0.84 (0.46, 0.92)	0.82 (0.70, 0.91)
GGO	0.96 (0.91, 1.00)	0.92	1.00 (0.74, 1.00)	0.92 (0.78, 0.98)	1.00 (0.89, 1.00)	1.00 (0.89, 1.00)	0.94 (0.83, 0.99)
Consolidation	0.68 (0.55, 0.81)	0.64	1.00 (0.48, 1.00)	0.36 (0.13, 0.65)	1.00 (0.48, 1.00)	1.00 (0.48, 1.00)	0.53 (0.29, 0.76)

Table 4. (Continue). The predictive power of study variables for prediction of vital status

Variables	AUC (95% CI)	Cut-off	SE (95% CI)	SP (95% CI)	PPV (95% CI)	NPV (95% CI)	Accuracy 95% CI)
Nodular	0.47 (0.44, 0.50)	0.28	1.00 (0.74, 1.00)	0.00 (0.00, 0.06)	NA (0.00, 1.00)	NA (0.00, 1.00)	0.78 (0.66, 0.87)
Highly Suggestive	0.34 (0.23, 0.44)	0.28	1.00 (0.74, 1.00)	0.00 (0.00, 0.06)	NA (0.00, 1.00)	NA (0.00, 1.00)	0.50 (0.38, 0.62)
Inconsistent	0.56 (0.52, 0.61)	0.30	1.00 (0.74, 1.00)	0.13 (0.05, 0.24)	1.00 (0.62, 1.00)	1.00 (0.62, 1.00)	0.28 (0.18, 0.40)
Indeterminate	0.51 (0.42, 0.59)	0.90	0.08 (0.00, 0.38)	0.93 (0.83, 0.98)	0.83 (0.10, 0.95)	0.83 (0.10, 0.95)	0.82 (0.71, 0.91)
PCR	0.36 (0.21, 0.50)	0.20	1.00 (0.63, 1.00)	0.00 (0.00, 0.09)	NA (0.00, 1.00)	NA (0.00, 1.00)	0.16 (0.07, 0.30)
Sex	0.52 (0.36, 0.68)	0.30	0.50 (0.21, 0.79)	0.54 (0.40, 0.67)	0.83 (0.57, 0.90)	0.83 (0.57, 0.90)	0.82 (0.71, 0.91)
Fever	0.55 (0.37, 0.72)	0.43	0.55 (0.23, 0.83)	0.55 (0.39, 0.70)	0.82 (0.54, 0.90)	0.82 (0.54, 0.90)	0.55 (0.40, 0.68)
Cough	0.58 (0.40, 0.75)	0.41	0.55 (0.23, 0.83)	0.60 (0.44, 0.75)	0.84 (0.57, 0.91)	0.84 (0.57, 0.91)	0.59 (0.45, 0.72)
Dyspnea	0.41 (0.23, 0.58)	0.35	1.00 (0.72, 1.00)	0.00 (0.00, 0.08)	NA (0.00, 1.00)	NA (0.00, 1.00)	0.38 (0.25, 0.52)
Smoke	0.44 (0.32, 0.57)	0.17	1.00 (0.72, 1.00)	0.00 (0.00, 0.08)	NA (0.00, 1.00)	NA (0.00, 1.00)	0.22 (0.12, 0.36)
Axial	0.49 (0.46, 0.51)	0.33	1.00 (0.74, 1.00)	0.00 (0.00, 0.09)	NA (0.00, 1.00)	NA (0.00, 1.00)	0.75 (0.61, 0.86)
Peribronchovascular	0.54 (0.46, 0.62)	1.00	0.08 (0.00, 0.38)	1.00 (0.91, 1.00)	0.78 (0.08, 1.00)	0.78 (0.08, 1.00)	0.77 (0.63, 0.87)
Diffuse	0.69 (0.53, 0.85)	0.51	0.58 (0.28, 0.85)	0.80 (0.64, 0.91)	0.86 (0.64, 0.94)	0.86 (0.64, 0.94)	0.77 (0.63, 0.87)
Pleural effusion	0.68 (0.53, 0.83)	0.71	0.42 (0.15, 0.72)	0.95 (0.85, 0.99)	0.88 (0.65, 0.97)	0.88 (0.65, 0.97)	0.82 (0.71, 0.91)
PHTN	0.51 (0.42, 0.59)	0.50	0.08 (0.00, 0.38)	0.93 (0.83, 0.98)	0.83 (0.10, 0.95)	0.83 (0.10, 0.95)	0.82 (0.71, 0.91)

Abbreviation: Area under curve (AUC), sensitivity (SE), specificity (SP), positive predictive value (PPV), negative predictive value (NPV)

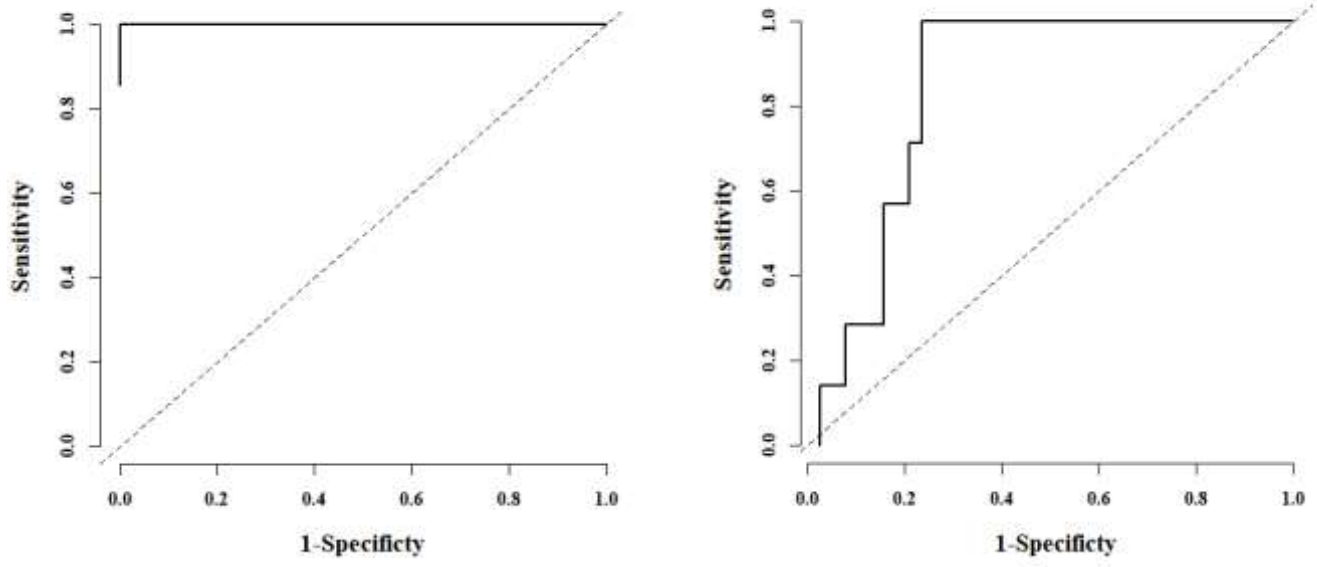

A) B)

Figure 1. The ROC curve for predicting vital status using A) GGO, LDH, Hb, Age, and Pleural effusion, B) LDH, Hb, Age, and Pleural effusion

Discussion

This retrospective study evaluated chest CT scan features as well as clinical presentation and laboratory data in COVID-19 recovered and dead patients hospitalized in a multicenter health system in Tehran-Iran during the first pandemic period.

Male sex is more than female in our cases, as noted in previous studies, showed an association between sex and mortality[20-22]. Another study showed that women were less susceptible to viral infection than men, possibly due to X chromosome protection and sex hormones [23].

The results showed dyspnea as the most common symptom in death cases, more than fever, cough, and fatigue. These three most common symptoms were mentioned in a meta-analysis study, which reported dyspnea prevalent about 21.4% [16].

The average body temperature was 37.48 ±0.8˚c at the initial physical examination in this study. Another study showed an association of fever and dyspnea with mortality[20].

Gastrointestinal symptoms like anorexia, nausea/vomiting, and general abdominal pain are also common in our cases compared with smell and taste disturbance, headache, sore throat, and rhinorrhea (these symptoms were rare in our cases).

A systematic review showed dyspnea, fever, headache, and myalgia proportions were lower in the mortality group with statistical significance for fever and dyspnea. This study also noted a higher proportion of diarrhea, nausea, and vomiting in the mortality group[22].

Up to 90% of death cases had co-morbidity like hypertension (HTN) as most common in this study. It is similar to the systematic review, which noted hypertension and diabetes mellitus (DM) as the most common co-morbidities[16]. Although, cancer and ischemic heart disease (IHD) are more common from diabetes in our patients.

A physiological study has noted HTN as the most common COVID-19 co-morbidity. It was due to the plasmin (ogen) process, such as other underlying conditions like DM, IHD, chronic kidney disease, and cerebrovascular disease which enhance the virulence of COVID-19 by cleaving its spike proteins[18].

White blood cell (WBC) count and neutrophil percentage are high in our study, in addition to low lymphocyte percentage. It is similar to the previous studies; a retrospective study demonstrated WBC count, and neutrophil percentage was higher and lymphocyte percentage lower in the severe group in comparison with mild disease group[17].

Inflammatory markers and enzymes (like ESR, CRP, LDH, ALT, and AST) were at high levels in our study. The high levels of these markers were noted by another study to multiple organ injuries in severe COVID-19 cases[19, 22].

Severe cases have dramatically increased levels of fibrinogen and INR, indicating a hypercoagulable state in the prior mentioned study (19, 22) similar to our patients with average INR=1.36±0.59.

ARDS is late complications before death, similar to a prior study[16]. However, acute kidney injury (AKI) is also represented in 10% of our cases. Three cases experience cardiac arrhythmia and arrest as the late complication. Some studies explained cardiac injury as a common condition among hospitalized patients with COVID-19 and its association with a higher risk of in-hospital mortality[24, 25].

Chest CT scans of death cases showed Ground glass opacity still the most frequent pattern, however, consolidation seems to be more frequent. Although, a study demonstrated an increase in the consolidation component of lesions, indicating the extension of the disease course and deterioration of the lesion, which were correlated to the pathological characteristics of severe patients[28]. Crazy paving was the third typical pattern. Involvement percentages had higher scores with dominantly lower lobes involvement. There was no normal chest CT scan among our patients, whereas there were a few chests CT scans with abnormal but inconsistent features for COVID-19.

One study result mentioned Ground glass opacities were predominant in the early phase (≤ 7 days since symptoms' onset), while crazy-paving pattern, consolidation, and fibrosis characterized late-phase disease (> 7 days). Also, CT score was significantly higher in critical and severe than in mild stages of COVID-19 [26].

There were three patients with cavitary involvement in death cases, whereas it was reported rarely in previous studies, a case report[27]. Pleural effusion prevalence was 38.6% in death cases.

There was no statistically significant difference in the affected segment of lung lobes between deceased and recovered patients. Also, the prevalence of some patterns, including consolidations and nodules were more in the deceased group.

Another study on CT scan images of 55 admitted patients demonstrated that right and left lower lobes were the most commonly affected lobes[29]. Results of a meta-analysis on 2,738 participants also showed RLL and left lower lobe (LLL) had the most affected lung lobes (87.21% and 81.41%, respectively)[30].

The GGO pattern is a frequent finding among different patterns[29, 31-34]. Kunhua et al. demonstrated that some patterns like linear opacities, bronchial wall thickening, lymphadenopathy, and pleural/pericardial effusion were more frequent in CT imaging of severely ill patients[33]. These findings are according to our results in which the architectural distortion, parenchymal band, pulmonary cavity, and pleural/pericardial effusion were only found in the deceased group. The pattern of distribution in our patients was similar to 236 hospitalized Italian patients in which diffuse and peripheral patterns were the most common ones[35].

A multicenter retrospective cohort study from showed that lymphadenopathy and pleural effusion with an incidence rate of 4.9% and 7.2% of participants, ordinary are infrequent patterns[36]. Also, the pulmonary nodules, cavities, lymphadenopathy, and pleural effusion in our sample are compatible with some other studies[37-39]. Furthermore, reticulation, cavitation, pleural effusion, bronchiectasis, and lymphadenopathy were rare occurrences in COVID-19 patients[41].

The fibrous lesions and fibrosis stripes were also other patterns that were reported in some CT images[40-41]. Siyao et al.[42] reported that 44.8% and 36.8% of discharged patients had fibrous lesions and fibrosis stripes, respectively, are in accordance with our results that pulmonary fibrosis was only found among recovered participants. In addition, this study revealed that fibrosis stripes take a longer time to disappear in comparison with GGO and fibrosis[42].

A systematic review and meta-analysis of 15 retrospective studies including 2,451 patients with COVID-19 revealed that the crazy-paving pattern is a significantly more common pattern in severe than non-severe patients (OR= 0.22 (95% CI: 0.11-0.44), p-value= 0.04)[43]. But, there was not any significant difference between recovered and deceased groups. Comparing the number of included participants in our study with the previous meta-analysis, it seems that the crazy-paving pattern might be used as an indicator of severity in large populations.

There were some limitations in the study. One, we included patients in one center, while the results might be more reliable if we engaged other national or international centers. Two, we assessed pulmonary radiological features and did not evaluate extra pulmonary manifestations[44]. Three, we did not include CT images of outpatients in the study. Four, we evaluated the initial CT images of the participant in the analysis, and the CT images during the natural history of the disease were not included so we might miss some patterns[45]. Five, we did not assess some patterns and signs such as tree-in-bud, pleural thickening, hydrothorax, sub pleural linear opacity, cystic change, and bronchial dilation. Six, we did not adjust the effects of comorbidities like pulmonary hypertension on the CT manifestations in these patients[46].

In summary, this study revealed CT feature parameters as well as clinical and laboratory markers, through two groups of death and survived COVID-19 cases, torich prognostic factors.

Conclusion

Our results show dyspnea as the most common symptom in death cases, gastrointestinal symptoms like anorexia, nausea/vomiting, and general abdominal pain are also common. Up to 90% of death cases had co-morbidity, which hypertension (HTN) is the most, and ARDS is near all patient's late complications before death. Inflammatory markers and coagulability state are high. Ground glass opacity was the most frequent pattern; however, consolidation seems to be more frequent than prior studies. Lesions distribution was dominantly diffuse than peripheral distribution; LLL and RLL were the most. The results of study show that chest CT imaging can help physicians to determine the severity of COVID-19. Also, it suggests that some CT patterns, including high score GGO, pleural/pericardial effusion, and pulmonary HTN can be predictors of poor prognosis. Furthermore, bronchiectasis, vascular enlargement, pulmonary mass, and lymphadenopathy were rare and might decrease the probability of COVID-19. The prediction power of some variables was significant. The highest AUCs were observed for variables of GGO pattern, age, lymphocyte count, Creatinine, CRP, LDH, and Systolic Blood Pressure.

Further large-scale multicenter retrospective and prospective studies on CT scan features of COVID-19 in addition to systematic review and meta-analysis of current evidence can help clinicians diagnose and determine the prognosis of COVID-19 based on chest clinical, para clinical data, and CT scan.

Acknowledgments

None

Conflict of Interest Disclosures

The authors declared no potential conflict of interests with respect to the research, authorship, and /or publication of this article.

Funding Sources

The authors received no financial or funding support for the research.

Authors' Contributions

All authors pass the four criteria for authorship contribution based on the international committee of medical journal editors (ICMJE) recommendations.

Ethical Statement

This study was approved by ethical committee of Shahid Beheshti University of Medical Sciences, Tehran, Iran.

References

1. S. Su, G. Wong, W. Shi, et al. Epidemiology, genetic recombination, and pathogenesis of coronaviruses. Trends Microbiol, 24 (2016), pp. 490-502

2. J.T. Wu, K. Leung, G.M. Leung. Nowcasting and forecasting the potential domestic and international spread of the 2019-nCoV outbreak originating in Wuhan, China: a modelling study. Lancet, 395 (10225) (2020), pp. 689-697

3. P Zhou, L Yang X, G Wang X, et al. A pneumonia outbreak associated with a new coronavirus of probable bat origin. Nature, 579 (7798) (2020), pp. 270-273

4. Li Y, Xia L. Coronavirus disease 2019 (COVID-19): role of chest CT in diagnosis and management. American Journal of Radiology. Am J Roentgenol:1–7. (2020)

5. World Health Organization website (2003) Summary of probable SARS cases with onset of illness from 1 November 2002 to 31 July 2003. World Health Organization, Geneva Available via http://www.who.int/csr/sars/country/table2004_04_21/en/. Accessed 15 Mar 2020

6. World Health Organization website (2019) Middle East respiratory syndrome coronavirus (MERS-CoV). World Health Organization, Geneva Available via http://www.who.int/emergencies/mers-cov/en/. Accessed 15 Mar 2020

7. Yang XB, Yu Y, Xu JQ et al. Clinical course and outcomes of critically ill patients with SARS-CoV-2 pneumonia in Wuhan, China: a single-centered, retrospective, observational study. Lancet Respiratory Medicine. 2020

8. Coronavirus disease (COVID-19) Situation Report–178; Data as received by WHO from national authorities by 10:00 CEST, 16July2020

9. https://www.who.int/docs/default-source/coronaviruse/situation-reports/20200716-covid-19-sitrep-178.pdf?sfvrsn=28ee165b_2

10.Long C, Xu H, Shen Q, et al. Diagnosis of the Coronavirus disease (COVID-19): rRT-PCR or CT? European Journal of Radiology. 2020 May; 126:108961.

11. Fang Y, Zhang H, Xie J, et al. Sensitivity of Chest CT for COVID-19: Comparison to RT-PCR. Radiology. 2020 Feb 19:200432

12. Ai T, Yang Z, Hou H, et al. Correlation of Chest CT and RT-PCR Testing in Coronavirus Disease 2019 (COVID-19) in China: A Report of 1014 Cases. Radiology. 2020 Feb 26:200642

13. Rodriguez-Morales AJ, Cardona-Ospina JA, Gutiйrrez-Ocampo E, et al. Clinical, laboratory and imaging features of COVID-19: A systematic review and meta-analysis. Latin American Network of Coronavirus Disease 2019-COVID-19 Research (LANCOVID-19). Travel Med Infect Dis. 2020 Mar-Apr; 34:101623

14. Frater JL, Zini G, d'Onofrio G, et al. COVID-19 and the clinical hematology laboratory. Internal Journal of Laboratory Hematology. 2020 Jun

15. Zhang JJ, Cao YY, Tan G, et al. Clinical, radiological and laboratory characteristics and risk factors for severity and mortality of 289 hospitalized COVID-19 patients. Allergy. 2020 Jul 14

16. Yong Hu, Jiazhong Sun, Zhe Dai, et al. Prevalence and severity of corona virus disease 2019 (COVID-19): A systematic review and meta-analysis. Journal of Clinical Virology 127 (2020) 104371

17. Chi Zhang1†, Ling Qin1†, Kang Li1†, et al. A Novel Scoring System for Prediction of Disease Severity in COVID-19. cellular-and-infection-microbiology, published 05 june 2020

18. Hong-Long Ji, Runzhen Zhao, Sadis Matalon, et al. Elevated Plasmin(ogen) as a Common Risk Factor for COVID-19 Susceptibility. Physiological Review 100: 1065–1075, 2020 First published March 27, 2020

19.HaijunWang, ShanshanLuo ,YinShen, et al. Multiple Enzyme Release, Inflammation Storm and Hypercoagulability are Prominent Indicators for Disease Progression in COVID-19:A Multi-centered, Correlation Study with CT Imaging Score. THE LANCET Infectious Disease -D-20-00537

20. panelJ.Zhang1†X. Wang2†X. Jia1J.et al. Risk factors for disease severity, unimprovement, and mortality in COVID-19 patients in Wuhan, China. Clinical Microbiology and Infection, Volume 26, Issue 6, June 2020, Pages 767-772

21. Yan Li, Zhenlu Yang, Tao Ai et al. Association of "initial CT" findings with mortality in older patients with coronavirus disease 2019 (COVID-19). European Radiology Published: 10 June 2020

22. ZhaohaiZhengab, FangPenga, BuyunXua, et al. Risk factors of critical & mortal COVID-19 cases: A systematic literature review and meta-analysis. Journal of Infection, Volume 81, Issue 2, August 2020, Pages e16-e25

23. Shani Talia Gal-Oz, Barbara Maier, Hideyuki Yoshida, et al. ImmGen report: sexual dimorphism in the immune system transcriptome. Nature Communications volume 10, Article number: 4295 (2019)

24.Shaobo Shi, Mu Qin, Bo Shen, et al. Association of Cardiac Injury with Mortality in Hospitalized Patients with COVID-19 in Wuhan, China. JAMA Cardiology. 2020 Mar 25;5(7):802-810.

25. Ahmed M A Shafi , Safwan A Shaikh , Manasi M Shirke , et al. Cardiac manifestations in COVID-19 patients-A systematic review. Journal of Cardiology Surgury. 2020 Aug;35(8):1988-2008.

26. Marco Francone , Franco Iafrate , Giorgio Maria Masci ,et al. Chest CT score in COVID-19 patients: correlation with disease severity and short-term prognosis. European Radiology journal. 2020 Jul 4;1-10.

27. Ying Chen, Wanling Chen, Jiansheng Zhou, et al. Large pulmonary cavity in COVID-19 cured patient case report. Ann Palliat Med. 2020 Jun 9; apm-20-452.

28. Dong Sun, MD, Xiang Li, MD, Dajing Guo, PhD, et al. CT Quantitative Analysis and Its Relationship with Clinical Features for Assessing the Severity of Patients with COVID-19. Korean Journal of Radiology. 2020 Jul;21(7):859-868. English.

29. Ashraf MA, Shokouhi N, Shirali E, Davari-tanha F, Memar O, Kamalipour A, et al. COVID-19 in Iran, a comprehensive investigation from exposure to treatment outcomes. medRxiv. 2020:2020.04.20.20072421.

30. Bao C, Liu X, Zhang H, Li Y, Liu J. Coronavirus Disease 2019 (COVID-19) CT Findings: A Systematic Review and Meta-analysis. J Am Coll Radiol. 2020;17(6):701-9.

31. Javanbakht M, Jafari R, Mesri M, Izadi M, Saadat SH. Chest Computed Tomography Findings in COVID-19 Pneumonia from Tehran, Iran. Open Access Macedonian Journal of Medical Sciences. 2020;8(T1):82-3.

32. Masoud N-V, Neda K, Akbar S, Pouya B, Zahra S, Erfan Ahmadi A, et al. Clinical Characteristics of Fatal Cases of COVID-19 in Tabriz, Iran: An Analysis of 111 Patients. Advanced Journal of Emergency Medicine. 2020;0(0).

33. Li K, Wu J, Wu F, Guo D, Chen L, Fang Z, et al. The Clinical and Chest CT Features Associated with Severe and Critical COVID-19 Pneumonia. Invest Radiol. 2020;55(6):327-31.

34. Zhang J-j, Dong X, Cao Y-y, Yuan Y-d, Yang Y-b, Yan Y-q, et al. Clinical characteristics of 140 patients infected with SARS-CoV-2 in Wuhan, China. Allergy. 2020;75(7):1730-41.

35. Colombi D, Bodini FC, Petrini M, Maffi G, Morelli N, Milanese G, et al. Well-aerated Lung on Admitting Chest CT to Predict Adverse Outcome in COVID-19 Pneumonia. Radiology. 2020;296(2): E86-E96.

36. Yang W, Cao Q, Qin L, Wang X, Cheng Z, Pan A, et al. Clinical characteristics and imaging manifestations of the 2019 novel coronavirus disease (COVID-19): A multi-center study in Wenzhou city, Zhejiang, China. J Infect. 2020;80(4):388-93.

37. Chung M, Bernheim A, Mei X, Zhang N, Huang M, Zeng X, et al. CT Imaging Features of 2019 Novel Coronavirus (2019-nCoV). Radiology. 2020;295(1):202-7.

38. Xu X, Yu C, Qu J, Zhang L, Jiang S, Huang D, et al. Imaging and clinical features of patients with 2019 novel coronavirus SARS-CoV-2. Eur J Nucl Med Mol Imaging. 2020;47(5):1275-80.

39. Li X, Zeng W, Li X, Chen H, Shi L, Li X, et al. CT imaging changes of corona virus disease 2019(COVID-19): a multi-center study in Southwest China. J Transl Med. 2020;18(1):154-.

40. Pan Y, Guan H, Zhou S, Wang Y, Li Q, Zhu T, et al. Initial CT findings and temporal changes in patients with the novel coronavirus pneumonia (2019-nCoV): a study of 63 patients in Wuhan, China. European Radiology. 2020;30(6):3306-9.

41. Dai H, Zhang X, Xia J, Zhang T, Shang Y, Huang R, et al. High-resolution Chest CT Features and Clinical Characteristics of Patients Infected with COVID-19 in Jiangsu, China. International Journal of Infectious Diseases. 2020; 95:106-12.

42. Du S, Gao S, Huang G, Li S, Chong W, Jia Z, et al. Chest lesion CT radiological features and quantitative analysis in RT-PCR turned negative and clinical symptoms resolved COVID-19 patients. Quant Imaging Med Surg. 2020;10(6):1307-17.

43. Zheng Y, Wang L, Ben S. Meta-analysis of chest CT features of patients with COVID-19 pneumonia. Journal of Medical Virology. 2020; n/a(n/a).

44. Behzad S, Aghaghazvini L, Radmard AR, Gholamrezanezhad A. Extrapulmonary manifestations of COVID-19: Radiologic and clinical overview. Clinical Imaging. 2020; 66:35-41.

45. Sirous J, Mohammadreza T, Sahereh E, Farnaz A, Armin A, Esmaeil M, et al. CT-scan Findings of COVID-19 Pneumonia Based on the Time Elapsed from the Beginning of Symptoms to the CT Imaging Evaluation: A Descriptive Study in Iran. Romanian Journal of Internal Medicine. 2020(0):000010247820200019.

46. Dong C, Zhou M, Liu D, Long X, Guo T, Kong X. Diagnostic Accuracy of Computed Tomography for Chronic Thromboembolic Pulmonary Hypertension: A Systematic Review and Meta-Analysis. PLOS ONE. 2015;10(4): e0126985.